Bioinspired Functional Catechol Derivatives Through Simple Thiol Conjugate Addition

Juan Mancebo-Aracil,*[a][b] Carolina Casagualda,[c] Miguel Ángel Moreno-Villaécija,[a] Fabiana Nador,[b] Javier García-Pardo,[a] Antonio Franconetti-García,[c] Félix Busqué,[c] Ramon Alibés,[c] María José Esplandiu,[a] Daniel Ruiz-Molina,[a] Josep Sedó-Vegara*[a]

Abstract: The combination of the surface-adhesive properties of catechol rings and functional moieties conveying specific properties is very appealing to materials chemistry, but the preparation of catechol derivatives often requires elaborate synthetic routes to circumvent the intrinsic reactivity of the catechol ring. In this work, functional catechols are synthesized straightforwardly using the bioinspired reaction of several functional thiols with *o*-benzoquinone. With one exception, the conjugated addition of the thiol takes place regioselectively at the 3-position of the quinone, and is rationalized by DFT calculations. Overall, this synthetic methodology is shown to provide a general and straightforward access to functional and chain-extended catechol derivatives, which are later put to the test with regard to their hydro/oleophobicity, colloidal stability, fluorescence and metal-coordinating capabilities in proof-of-concept applications.

Introduction

Biomimetic analogues of mussel-adhesive foot proteins (mfp's) have been the subject of intensive research over the past years. The remarkable ability of these marine organisms to cling, not only to rocky surfaces native to their environment, but virtually to any surface (even low-fouling materials), has been largely attributed to the presence of a significant fraction of catecholic amino acid L-3,4-dihydroxyphenylalanine (L-DOPA) in the sequence of the mfp's.[1] Hence, an increasing number of works have focused on the synthesis of new bioinspired catechol-based molecules and polymers, which have shown to be useful for manufacturing water-resistant adhesives,[2] protective layers,[3] and primers for functional adlayers and nanoscale coatings,[4] among others.[5] In a previous report,[6a] we presented a successful design for catechol-capped functional coatings, based on the synthesis of catechol derivatives bearing a specific functional moiety in the 4- position, followed by their polymerization in an excess of hydroalcoholic ammonia. This design ensured both a robust (non-hydrolyzable) attachment of the functional moiety to the catechol ring, and an accurate control of the degree of functionalization of the final material. Nevertheless, a relatively lengthy synthetic route was needed to afford the respective catecholic derivatives, comprising protection/deprotection of the catechol ring, relatively harsh reaction conditions, and overall poor atom economy. These drawbacks limited the scope of application of this route, which could not satisfy the need for a general approach to the preparation of functional catechol derivatives.

Despite the growing interest for the synthesis of functionalized catechols, few other synthetic methodologies affording robust attachment of functional chains to simple catechols have been described in the literature. For example, the electrophilic aromatic substitution on catecholic derivatives using electrophile species allows the introduction of different alkyl and acyl substituents on this ring, either in 3- or 4- position. However, in most examples this methodology is only applied to specific cases yielding mixtures of 3- and 4- alkylated catechols,[7] or mixtures of mono- and dialkylated products.[8] Examples where a acylated[9] or single alkylated[10] catechol is obtained are scarce. On the other hand, the oxidation of a starting catechol to the corresponding *o*-quinone and subsequent conjugated nucleophilic addition of a thiolated derivative should provide a straightforward way to attach substituents of choice to catechol rings via non-hydrolyzable *S*-aryl linkages. Indeed, the complex interplay between thiol groups and *o*-quinones is known to play important roles in biological contexts; for instance, it has been invoked as a repair mechanism in mussel foot proteins, where catechol moieties in L-DOPA units undergo oxidation in their natural environment with a concomitant loss of the adhesive capabilities. In the presence of free thiols of cysteine units in the protein sequence, redox exchanges, as well as conjugate addition reactions restore the structure of the catechol ring, while at the same time increasing the bulk cross-linking density.[11] Other relevant examples are evinced by the biosynthesis of pheomelanin and the neutralization of *o*-quinoid species derived from catechol estrogens by conjugation with cysteine free thiols, which is thought to be the main mechanism behind the protective role of this amino acid against highly electrophilic carcinogenic metabolites.[12] So far, thiol-quinone conjugation for synthetic purposes has been shown for cysteine units, thiophenol, mercaptobenzothiazole and ethanethiol to different catechol derivatives,[13],[14], but to the best of our knowledge, no general approach for the preparation of simple catechol S-

[a] J. Mancebo-Aracil, J. Sedó-Vegara, M. A. Moreno-Villaécija, J. García-Pardo, María José Esplandiu, D. Ruiz-Molina
Catalan Institute of Nanoscience and Nanotechnology (ICN2), CSIC and BIST
Campus de la UAB - 08193 Bellaterra (Spain)
E-mail: josep.sedo@icn2.cat
[b] J. Mancebo-Aracil, F. Nador
Instituto de Química del Sur-INQUISUR (UNS-CONICET)
Universidad Nacional del Sur
Av. Alem 1253, 8000 Bahía Blanca, Buenos Aires (Argentina)
E-mail: juan.mancebo@uns.edu.ar
[c] C. Casagualda, A. Franconetti-García, F. Busqué, R. Alibés
Departament de Química
Universitat Autònoma de Barcelona (UAB)
Campus de la UAB - 08193 Bellaterra (Spain)

Supporting information for this article is given via a link at the end of the document.

functional derivatives for potential applications in materials science has been reported.

Here we report a systematic and straightforward methodology for the synthesis of functional catechol derivatives by oxidation of the simplest catechol (pyrocatechol) to the corresponding *o*-quinone, followed by the conjugated nucleophilic addition of different thiol-capped reagents bearing functional substituents. Thiolated precursors were chosen for several reasons: they are widely available, they may be used either as simple functional moieties themselves or as chain-extenders, they provide robust aryl-*S* links to the pyrocatechol ring and, last but not least, optimal atom efficiency. Following this procedure, a wide variety of moieties, such as aliphatic, fluorinated, polyethylene glycol-bearing (PEGylated) chains, fluorescent tags and chain extenders, are introduced in the catecholic ring using a unified methodology. In order to showcase the usefulness of these catecol derivatives we present their use as coatings for the modification of the wettability of macroscopic surfaces, the stabilization of colloidal dispersions of nanoparticles in aqueous solutions, and the preparation of coordination ligands that serve as fluorescent markers for theranostic nanoparticles in biomedical applications.

Results and Discussion

The attachment of thiolated chains to pyrocatechol takes place in two stages. Pyrocatechol is first oxidized to *o*-benzoquinone. A thiol is subsequently added, undergoing nucleophilic attack to the quinoid ring. The reaction proceeds through a keto-enol intermediate that spontaneously tautomerizes into the substituted catecholic form (Scheme 1, top).

Optimization of the reaction. The thiol of choice for the study and optimization of the conjugate addition reaction was 1-octadecylthiol **1a**. The oxidation of pyrocatechol to the corresponding *o*-benzoquinone was carried out in water using a small excess of one equivalent of $NaIO_4$,[15] commonly used for the oxidative activation and cross-linking of catechol-based adhesives. Although the oxidation step proved to be reproducible with yields of pure *o*-benzoquinone around 75%, the instability of this compound prompted us to skip the isolation of the quinone altogether by extracting it into CH_2Cl_2, followed by the immediate addition of one equivalent of the thiol under argon. In line with two previous reports,[13c,f] a mixture of the desired mono-adduct **2a**, together with a significant amounts of the symmetrical bis-adduct **3a** and **1a**-disulfide were detected in the ^{1}H NMR spectrum of the reaction crude, with the molar ratio between **2a** and the sum of these two side-products being 1.1:1 (Table 1, entry 1). From a mechanistic point of view, the introduction of a second thiolated unit may be explained by assuming that a fraction of thiolated catechol **2a** is oxidized by unreacted *o*-benzoquinone to the corresponding thiolated *o*-quinone, which then becomes the substrate for a second conjugate addition. The concomitant production of significant amounts of **1a**-disulfide suggested that at least a certain amount of unreacted thiol **1a** also participates of redox-type side-reactions with *o*-quinoid species (Scheme 1). An overall picture of this seemingly simple reaction may be thus laid out, in which at least seven different species are coupled together by conjugate nucleophilic additions and redox exchanges (SM, Figure S1). In the former, *o*-quinones act as electrophilic counterparts for the nucleophilic thiol, whereas in the latter, the thiol reagent, and both pyrocatechol and thiolated catechols, act as reducing agents for both *o*-benzoquinone and thiolated *o*-quinones. Further support for this hypothesis was gained from non-aqueous cyclic voltammetry experiments on pyrocatechol and mono-adduct **2a**, showing peak oxidation potentials at *ca.* +1.4 V vs Ag/Ag^+ for both catecholic species (Fig. S5), With regard to regioselectivity, it was observed that the conjugated addition of **1a** took place essentially at the 3-position, since no traces of the 4-substituted derivative could be detected in the reaction crude. This result is consistent with previous reports on the selectivity of conjugated addition of thiol derivatives to different oxidized catechol derivatives.[16]

In order to improve the conversion of the addition reaction towards the mono-adduct **2a**, several changes in the reaction conditions were screened (Table 1, entries 2-14), and the progress of the reaction was followed by ^{1}H NMR spectroscopy of the reaction crude. Replacement of CH_2Cl_2 by other solvents led to lower conversion values of thiol **1a** (entries 2 & 3). Changes in the reaction temperature turned out to be detrimental to net conversion into **2a** (entries 4 & 5). The introduction of activators in the reaction mixture, either basic in order to increase the nucleophilic character of the thiol, or acidic in order to enhance the electrophilicity of the quinone system, were generally detrimental to the course of the reaction (1,8-Diazabicyclo[5.4.0]undec-7-ene (DBU), bis(trifluoromethane) sulfonamide (TFSI) or $Ti(BuO)_4$), or neutral at best (L-Proline), compared to activator-free reaction conditions (entries 6-9). The only exception was trifluoroacetic acid (TFA, entries 10-14), which was observed to enhance significantly the overall conversion of the thiol, as well as the production of the desired mono-adduct **2a,** already when the activator was present in sub-stoichiometric amounts. A favorable trend was observed by increasing the amount of TFA up to 3 eq (entry 12), which yielded a high overall conversion of the thiol (ca. 80%), and the highest mono-adduct content in the reaction mixture (>4:1 molar ratio), with higher activator loadings offering no significant advantage (entry 13). The use of a sub-stoichiometric amount of the thiol (0.75 eq) led to the highest overall conversion of thiol **1a**, but the reaction mixture showed a lesser content in mono-adduct **2a** (entry 14).

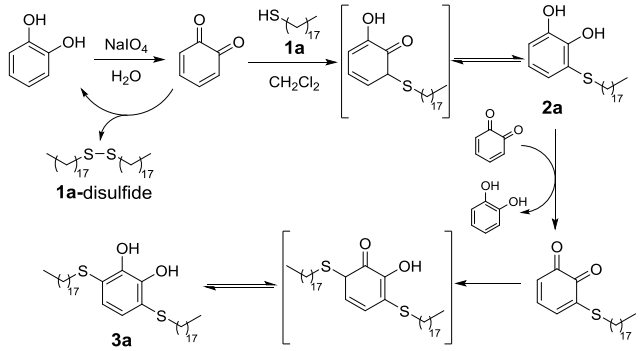

Scheme 1. Proposed mechanism for the obtention of mono- and bis-adducts of 1-octadecylthiol and pyrocatechol by combination of conjugate addition and redox reactions.

Table 1. Screening and optimization of the reaction conditions for octadecylthiol **1a**[a]

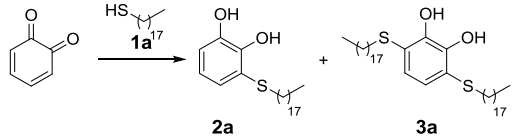

Entry	Solvent[a]	Activator	**1a** conv [e][f] (%)	**2a**[e] (%)	Molar ratio[e] **2a**:(**3a** + **1a**-disulfide)
1	CH_2Cl_2	-	65	15	1.1:1
2	*n*-hexane	-	80	15	0.4:1
3	*n*-hexane/ CH_2Cl_2 (5:1)	-	55	15	0.7:1
4	CH_2Cl_2[b]	-	70	15	0.6:1
5	CH_2Cl_2[c]	TFA, 1 eq	75	20	0.8:1
6	CH_2Cl_2	DBU, 0.1 eq	-	-	-
7	CH_2Cl_2	$Ti(BuO)_4$, 1 eq	-	-	-
8	CH_2Cl_2	TFSI, 1 eq	-	-	-
9	CH_2Cl_2	L-Pro, 1 eq	65	20	0.8:1
10	CH_2Cl_2	TFA, 0.2 eq	75	30	1.4:1
11	CH_2Cl_2	TFA, 1 eq	85	40	2.0:1
12	**CH_2Cl_2**	**TFA, 3 eq**	**80**	**55**	**4.3:1**
13	CH_2Cl_2	TFA, 5 eq	80	50	3.3:1
14	CH_2Cl_2[d]	TFA, 3 eq	>95	55	2.7:1

[a] General reaction conditions: 6h, room temperature, 1 eq of thiol **1a** (except where otherwise stated); [b] 0ºC; [c] reflux; [d] 0.75 eq **1a**; [e] Determined by ^{1}H NMR of the crude material; values referred to thiol **1a**; [f] **2a** + **3a** + **1a**-disulfide

Overall, the use of 3 eq of TFA in CH_2Cl_2 at room temperature offered the best balance between thiol conversion and mono-adduct purity (Table 1, entry 12). The suitability of these optimized conditions was confirmed with the isolation of mono-adduct **2a** after purification by column chromatography in 61% yield, which could be separated successfully from a lesser amount of bis-adduct **3a** (25%).

Scope of the reaction. The optimal reaction conditions for the model reaction (room temperature, 3 eq of TFA), were used for the conjugation of several thiol compounds (**1a-e**, Table 2), chosen to bear functional moieties of interest to materials chemistry. Together with the long alkyl thiol previously discussed (**1a**), a fluorinated (**1b**) and a PEGylated thiol (**1c**) were chosen for their potential ability to tune surface wettability and, in the latter case, in order to confer stability to nanoparticles in physiological media. On the other hand, mercaptobenzothiazole (**1d**) and a mercaptocoumarine (**1e**) were picked up to exemplify the coupling of thiolated heterocycles to catechol moieties.

Table 2. Synthesis of functional catechols.

Functional thiol	Catechol derivative[a]	
1a	**2a**, 61%	**3a**, 25%
1b	**2b**, 37%	**3b**, 16%
1c	**2c**, 56%	
1d	**2d**, 64%	
1e	**2e**, 45%	

[a] Yields referred to respective parent thiols after purification by column chromatography

The expected mono-adducts **2a-e** were thus obtained in moderate to high yields (37-64%). In the case of alkyl and

fluoroalkyl derivatives **2a** and **2b**, the corresponding bis-adducts **3a** and **3b** were isolated alongside as by-products of the synthesis, whereas in the other cases, only the intended mono-adducts (**2c**-**e**) could be purified from the reaction crude, and no traces from bis-adducts were observed. Overall, these results confirm that the optimized procedure may be generalized to obtain a wide variety of functional catecholic derivatives. With regard to the regioselectivity of the conjugate addition, and in agreement with a reported precedent using a different methodology,[14b] 2-mercaptobenzothiazole **1d** was the only thiol undergoing selective 1,4-addition to the 4- position, instead of the 1,6-addition to the 3- position of the ring observed for all the other thiols tested. Remarkably, this regioselectivity was observed to be extensive to the second conjugate addition, which was observed to take place selectively at the 6- position for compounds **3a** and **3b**.

The next step in this study was the conjugation of one or two pyrocatechol molecules to α,ω-dithiols **4a-d** bearing apolar alkyl chains (1,6-butanedithiol **4a** and 1,6-hexanedithiol **4b**), a polar moiety (2,2-(ethylenedioxy)diethanethiol) **4c**), and pendant hydroxyl groups (DL-dithiothreitol **4d**), in order to obtain catechol-thiol derivatives **5** and bis-catechol derivatives **6** (Table 3). In both families of compounds, the central chain was intended as a chain-extender in the catechol derivative, providing an adequate degree of flexibility, as well as enough spatial separation when needed, between the catechol moiety and either a second catechol moiety **6**, or a free thiol **5**. In the first case, bis-catechols **6** could be used as flexible bidentate ligands for coordination chemistry. In this regard, similar bis-catechol molecules have been used successfully by our group as ligands for the preparation of coordination polymer particles, as well as polydopamine-like gatekeeping coatings.[17] With regard to catechol-thiols **5**, the terminal thiol should allow further conjugation of the catechol-thiol to functional moieties bearing *electrophilic* reactive ends, such as vinyl, acrylate or isocyanate groups, thus providing an straightforward alternative route to functional catechols.

Using a pyrocatechol/dithiol 1:1 molar ratio, catechol-thiols **5a**-**d** were thus prepared by direct conjugation (Method A, see Experimental Section) in moderated yields ca. 35% (Table 3). Bis-catechol adducts **6a**-**6c** were also isolated from the reaction crude in low-to-moderate yields (11-36%). For cases for which the separation of **5**/**6** mixtures should turn out problematic, an alternative route (Method B) to catechol-thiols (**5**), comprising the selective protection and deprotection of a single thiol group, was also tested and exemplified for α,ω-dithiols **4b** and **4c** (Scheme 2, right). We first prepared and purified the corresponding monoacetylated thiols (**7b** and **7c**), and subsequently conjugated them to *o*-benzoquinone in order to obtain the respective chain-extended catechol thioacetates (**8b** and **8c**). Deprotection of these precursors in hydrochloric acid/methanol proceeded quantitatively, affording the pure catechol-thiols (**5b** and **5c**) in final overall yields that were slightly higher (41-43%) than those of the direct route.

Table 3. Synthesis of chain-extended catechol-thiols, bis-catechols and protected intermediates

α,ω-dithiol	Chain-extended catechol derivative[a][b]
4a	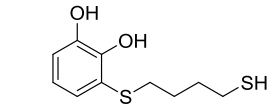 **5a**, 33%
	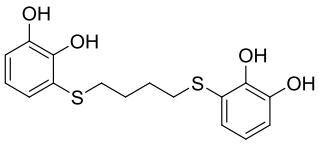 **6a**, 11%
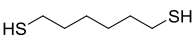 **4b**	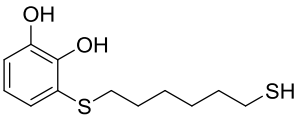 **5b**, 35% (43%)
	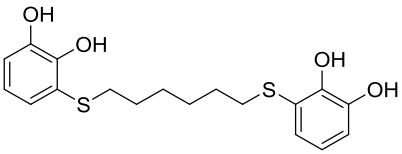 **6b**, 36%
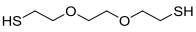 **4c**	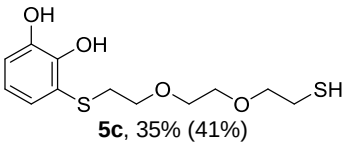 **5c**, 35% (41%)
	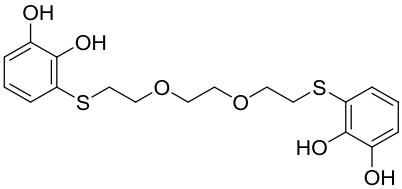 **6c**, 11%
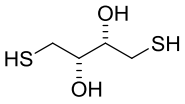 **4d**	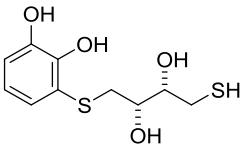 **5d**, 33%

[a] Yields referred to respective parent thiols after purification by column chromatography; [b] Yields reported for **5a**-**d** (Method A), and **5b**-**c** (Method B, between parentheses)

To show the feasibility of the functionalization of catechol-thiols (**5**) by conjugation of the free thiol with electrophilic moieties, two derivatives of compound **5b** were prepared. Firstly, this compound was selectively oxidized to the corresponding bis-catechol disulfide **9** with an equivalent of iodine (Scheme 3, left), in quantitative yield. It should be noted that, in contradistinction to the bis-catechol compounds **6** mentioned before, bis-catechol derivatives such as **9** include a central disulfide bridge, which is potentially cleavable. Remarkably, this oxidative coupling of thiols proceeded selectively in the presence of catechol rings, without the need of any additional protection/deprotection steps. Secondly, **5b** was derivatized in moderate yield (60%) into the corresponding fluorescent catechol derivative **10** by reaction with fluorescein 5(6)-isothiocyanate (FITC), a fluorescent marker commonly used in biomedical applications (Scheme 3, right). As in previous steps, the atom efficiency of the reactions to prepare derivatives **9** and **10** is optimal.

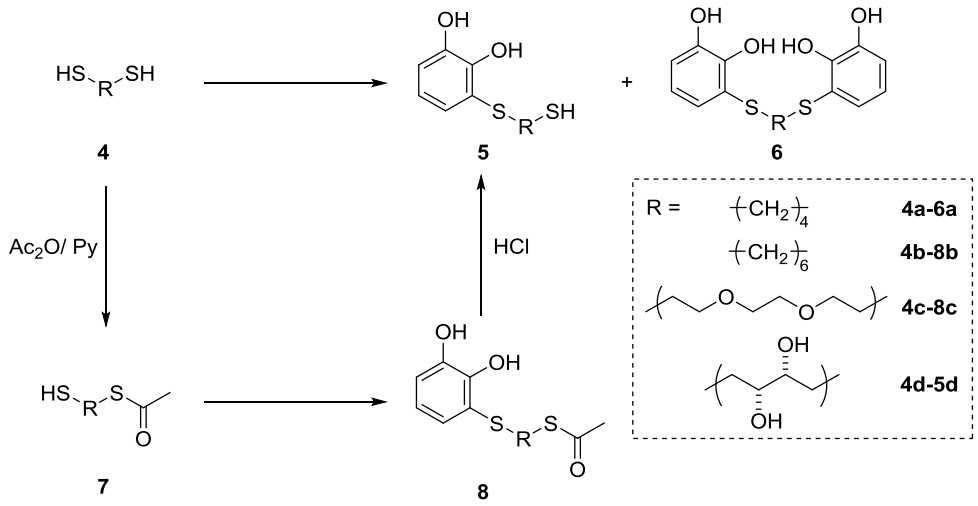

Scheme 2. Synthesis of chain-extended catechol derivatives (**5**, **6**) from α,ω-dithiols by direct conjugation (Method A), or conjugation sandwiched by selective protection/deprotection of one thiol group (Method B).

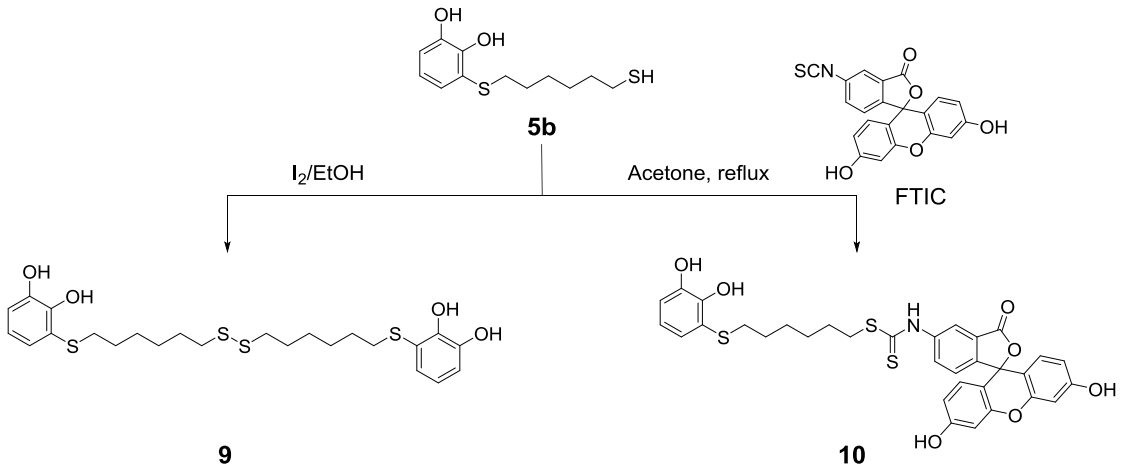

Scheme 3. Synthesis of bis-catechol disulfide **9** and chain-extended fluorescein derivative **10**.

Computational studies. In order to rationalize the origin of the observed regioselectivity of the conjugate addition, theoretical calculations were carried out at the PBE0-D3/def2-TZVP level of theory (see the experimental part for computational details). In general, the 1,6-conjugated additions are not favored because the largest coefficient of the LUMO orbital is located at the C-4 position.[18a] In our particular system, the C-4 carbon of *o*-benzoquinone also presented the largest coefficient. Moreover, molecular electrostatic potential (MEP) surface analysis of *o*-benzoquinone (Fig. 1) revealed a positively charged region on

the surface of both C-3 and C-4 carbons, with electrostatic potential values at van der Waals distances favoring the C-4 position (7.6 vs 15.0 kcal/(mol·e) for C-3 and C-4, respectively). In view of these considerations, the addition of the thiol derivative should be expected at C-4 position as a general rule. However, since with the exception of mono-adduct **1d**, experimental results for all the other functional thiols showed addition taking place *instead* at C-3, a more elaborate explanation was sought from calculations taking into account different feasible reaction pathways.

Taking a model compound (ethanethiol) as a model for **1a**, results suggested that the attack on the C-3 position is favored due to the incipient formation of a hydrogen bonding interaction between the thiol and one of the carbonyl groups of *o*-benzoquinone. In this regard, a non-covalent C=O···H-S contact was evinced both by atoms-in-molecules analysis (AIM, Fig. 1, left) and the non-covalent interaction plot (NCI, Fig. S2). Eventually, this interaction leads to the formation of a bond path interconnecting the S atom with both the carbonyl and the C-3 position (**TS_{HB}-C3**). It seems thus reasonable to assume that this network of interactions helps anchor the thiol group in the close vicinity of one of the carbonyl groups in early stages of the reaction, and thus drive the nucleophilic addition to the C-3 position.

Since regioselectivity on C-3 for **1a** was observed experimentally both in the absence of activators and in the presence of TFA, we estimated the energy profiles in both cases. Taking into account that *o*-benzoquinone is able to form parallel-displaced π-dimers (ΔE_{bind} = -5.5 kcal/mol), a second quinone molecule was incorporated in the calculations for the non-activated reaction. For **TS1a-C4**, this was necessary for the capture of the thiol proton. In these systems, an increase in the LUMO coefficient at C-3 further favored the 1,6 addition ($\Delta\Delta E$ = -6.3 kcal/mol). With regard to TFA-assisted transition states (**TS1a-C3^{TFA}** and **TS1a-C4^{TFA}**, Fig. S4), this activator facilitates the protonation of a carbonyl group, with the concomitant formation of a network of hydrogen bond-mediated interactions in both cases, favoring again the 1,6 addition ($\Delta\Delta E$ = -5.8 kcal/mol). The calculated energy for the final C-3 (**2a**) and C-4 (**2a-C4**) adducts was roughly very similar.

With regard to mercaptobenzothiazole **1d**, it has already been reported that this molecule exists essentially in the keto form (benzothiazoline-2-thione) in solution over a broad range of temperatures.[18b] Using our own calculation methodology, we evaluated the relative stability of both benzothiazoline-2-thione (*thioketo*-**1d**) and 2-mercaptobenzothiazole (*thioenol*-**1d**) tautomers. In agreement with the previous study, *thioketo*-**1d** was indeed predicted to be the most stable tautomer (-11.2 kcal/mol) in CH_2Cl_2, so we picked up this species for all energy profile calculations (Fig. 2).

Similarly to transition states for **1a**, TFA was shown to assist in the protonation of carbonyl groups and the establishment of complex networks of hydrogen bonds (this time around involving with the nitrogen-bound proton), but **TS1d-C4^{TFA}** ended up being significantly favored compared to **TS1d-C3^{TFA}** ($\Delta\Delta E$ = -11.8 kcal/mol). As with alkyl adducts, calculated energy differences between final regioisomers **2d** and **2d-C3** are minimal, so overall the structure and energy of transition states seems key to explaining the observed differences in regioselectivity.

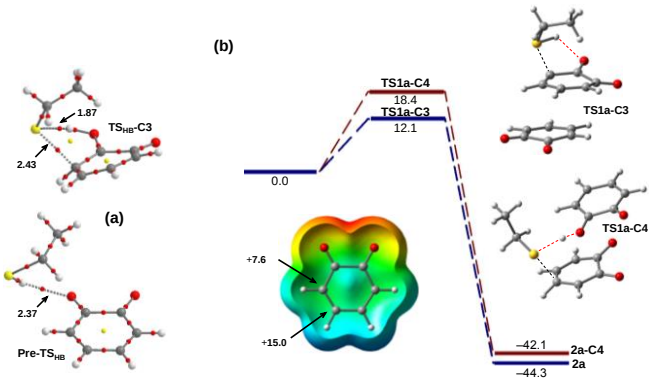

Figure 1. AIM analysis of bond critical points and paths showing hydrogen bonding interactions in the early stages of the reaction (left). MEP of *o*-benzoquinone plotted on the van der Waals surface, with energies of C-3 and C-4 carbons (center, bottom). Calculated energy profile and optimized TS structures for the non-activated addition of an aliphatic thiol to *o*-quinone at C-3 (dashed blue lines) and C-4 (dark red lines) positions, optimized at the PBE0-D3/def2-TZVP level. All energy values are relative to the reactants and are given in kcal/mol; distances given in Å.

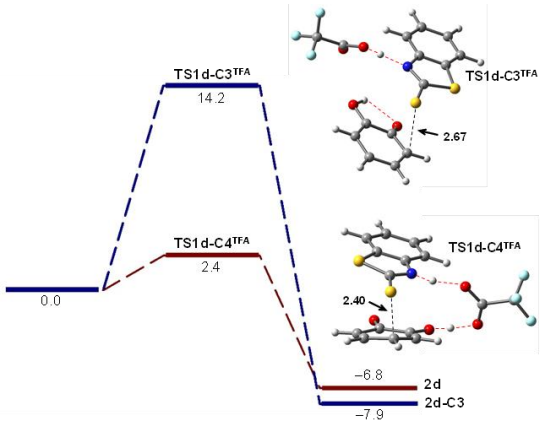

Figure 2. PBE0-D3/def2-TZVP optimized structures and energy profile for the addition of benzthiazoline-2-thione to *o*-quinone at C-3 (dashed blue lines) and C-4 (dark red lines) positions. Energies are given in kcal/mol and distances in Å. Hydrogen bonds in structures are highlighted by blue dashed lines.

Proof-of-concept examples. In order to show the potential usefulness of the functional catechols reported here, some of them were put to test as functional coatings for macro- and nanostructures and functional ligands for bioapplications.

First, alkylated mono- and bis-adducts **2a** and **3a,** polyfluoroalkyl homologues **2b** and **3b**, as well as polymers **p2a** and **p2b** derived from the aerobic oxidation products of **2a** and **2b**, were used to prepare hydro- and oleophobic coatings for macroscopic surfaces. From a structural point of view, it may be noted that the alkylated S-catechol mono-adduct (**2a**) is very similar to urushiol-type alkylcatechols, which are the main components of

traditional Japanese lacquered coatings.[19] For the preparation of **p2a** and **p2b**, we followed a procedure recently reported by us for the oxidative polymerization of 4-heptadecylcatechol.[5] Briefly, isopropanol solutions of each mono-adduct were mixed with an excess of aqueous ammonia and stirred in air at room temperature, yielding dark-brown precipitates that were extracted in apolar solvents, and further deposited on substrates by dip coating. Although the exact chemical composition of ammonia-oxidized catechol derivatives was not determined,[5] they are likely formed in a similar way to polydopamine and other melanin-like materials in general.[6] Presumably, after the oxidation of catechol moieties by atmospheric oxygen in moderately basic media, the corresponding *o*-quinone and semiquinone intermediates either couple directly, or through ammonia, which would act as a nucleophile on the reactive o-quinones thus formed, either through Michael addition or by direct attack on a quinoid carbonyl to form a Schiff base.[5] Regardless of the exact mechanism/s involved, because of the many potentially reactive positions involved, any combination of these reactions would be expected to eventually provide a certain degree of covalent linkage between catechol moieties, thus giving rise to a mixture of oligomeric/polymeric species bearing functional (in this particular case, hydrophobic) substituents.

TiO_2 surfaces and cotton cloth were dip-coated with solutions of alkyl (**2a**, **3a**) and polyfluoroalkyl (**2b**, **3b**) derivatives, as well as that of polymerized mono-adducts (**p2a**, **p2b**), and the corresponding static contact angles (SCA) were measured. For TiO_2 (Figure 3, top), results for water drops are virtually identical to each other, proving that all long-alkyl and polyfluoroalkylcatechols monomers and polymers reported here confer hydrophobicity to this metal oxide surface. Significant differences arose, however, after testing coated cotton samples.

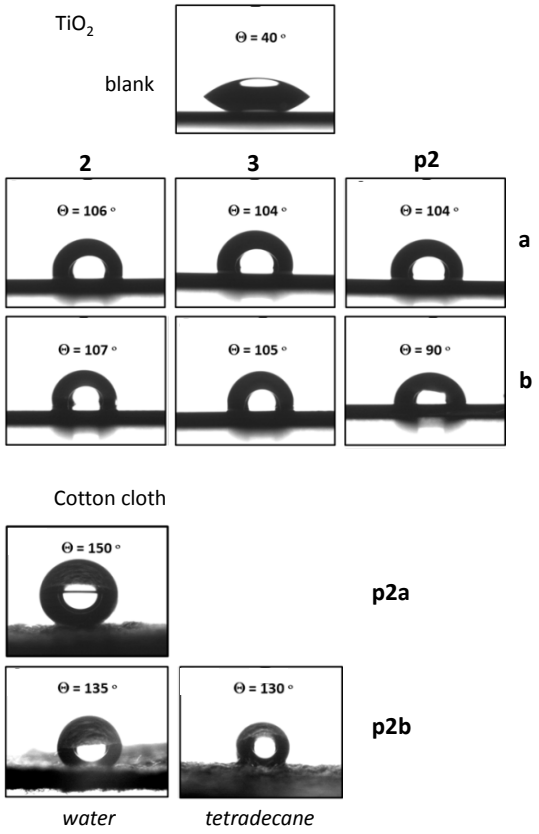

Figure 3. Static contact angles (SCA) of water drops on TiO_2 surfaces Uncoated TiO_2 blank; TiO_2 coated with alkylcatechol derivatives **2a**, **3a** and **p2a**, and polyfluoroalkyl catechol derivatives **2b**, **3b** and **p2b**. SCA of fluid drops on coated cotton coated with alkylated polymer **p2a** (water) and polyfluoroalkylated polymer **p2b** (water, tetradecane).

For non-polymeric catechol derivatives (**2a**, **3a**, **2b** and **3b**) no contact angle could be measured due fast water absorption by the textile. However, impregnation of cotton with **p2a** and **p2b** afforded hydrophobic coatings with high contact angle for water droplets (Figure 3, bottom). Particularly, the water CA of **p2a**-coated cotton (150º) turned out to be qualitatively similar to that reported by us for ammonia-polymerized 4-heptadecylcatechol (134º),[5b] and comparatively persistent. Moreover, for the polymerized polyfluorinated derivative **p2b**, the lack of wetting of the treated surface by tetradecane (CA = 130º) shows that this material is able to confer strong oleophobicity to the otherwise highly absorbent and hydrophilic cotton.

The ability of S-catechol derivatives to coat nanostructures was shown in a first example by polymerizing bis-catechol disulfide **9**, following an *in situ* protocol previously reported for the melanization of other bis-catechols intended as “plug” coatings for nanocarriers.[17b] Mesoporous silica nanoparticles (MSNs) were then suspended in a solution of polymer **p9** to carry out the deposition of the coating. Scanning transmission electron microscopy (STEM) images showed silica cores surrounded by a thick layer (ca. 200 nm) of the catecholic polymer, which was evinced in the energy-dispersive X-ray spectroscopy (EDX) line

scan by the presence of a significant amount of sulfur across the *whole* diameter of a coated particle, in contradistinction to the Si signal, which appeared circumscribed to its inner section, i.e. to the mineral core (Figure 4).

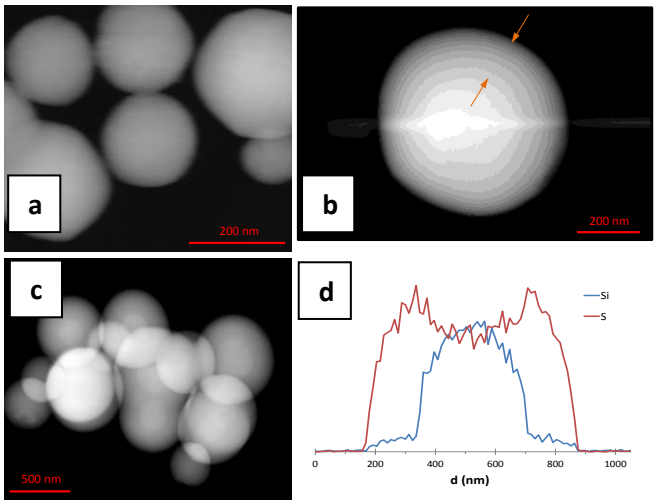

Figure 4. a) SEM image of uncoated mesoporous silica nanoparticles (MSNs); **b)** TEM image of a coated MSN singled out for EDX line scan, with arrows indicate the approximate edges of the coating; **c)** TEM image of MSNs coated with **p9**; **d)** EDX line scan profile.

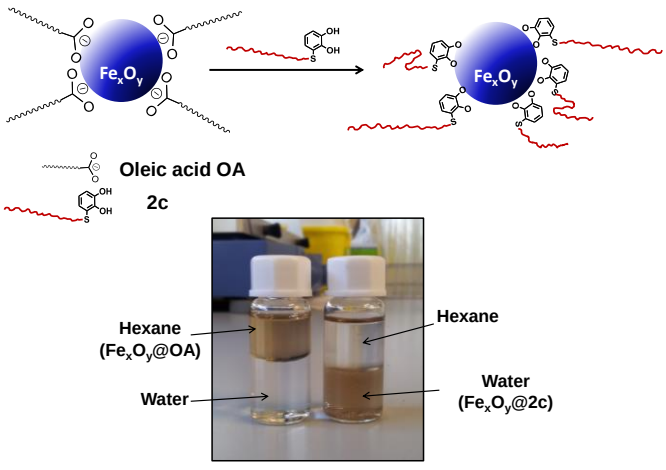

Figure 5. Stabilization of a colloidal dispersion of Fe_xO_y NPs in a *n*-hexane/water mixture as originally coated with oleic acid (left) and after treatment with PEGylated derivative **2c**.

In a second example, the colloidal stabilization capabilities of PEGylated catechol **2c** were explored by treating a *n*-hexane suspension of oleic acid-stabilized iron oxide nanoparticles (NPs) with a dichloromethane solution of this catechol derivative. After centrifugation, iron oxide nanoparticles were re-suspended in a water/*n*-hexane mixture. Whereas a control of the original NPs remained dispersed in the organic phase of the mixture after vigorous shaking, **2c**-coated NPs were readily transferred to the aqueous phase (Figure 5). This change in the wettability behavior is explained by the hydrophilic PEGylated derivative **2c** replacing the original (hydrophobic) oleic acid layer on the NPs. The comparatively higher affinity of catechol moieties for iron atoms is thought to be instrumental in this ligand displacement.

Finally, we tested the fluorescein-grafted derivative **10** as a fluorescent marker/ligand for the design of new theranostic nanocarriers. Firstly, coordination polymer nanoparticles (CPNPs) were prepared by using a previously reported generic protocol based on the fast-precipitation method.[17a] For this work, a Co^{II} salt was reacted with a combination of a bidentate scaffold ligand (1,4-bis(imidazol-1-ylmethyl)benzene (BIX)),[20] and two catechol derivatives - a catecholic prodrug moiety (L-DOPA methyl ester), and **10** -, both acting as monodentate ligands filling up the remainder of the metal coordination sphere (Scheme 4). **10**-containing nanoparticles of ca. 50 nm in diameter readily precipitated from the reaction crude. As evinced by their fluorescence emission spectrum (Figure 6, top), the marking capabilities of the parent fluorescent moiety were preserved after its incorporation in the coordination polymer. In order to test these properties in a bioassay, M17 neuroblastoma cells were incubated at 37 °C in the presence of **10**-marked CPNPs (50 µg/mL) for 6 hours. The *in vitro* internalization of the fluorescent nanoparticles was followed by confocal fluorescence microscopy, and their intracellular localization was checked by means of 3D image reconstructions (Figure 6, bottom), showing clusters of nanoparticles (green) located inside the cell cytoplasm, but outside the nucleus (blue) and lysosomes (red). This experiment qualitatively demonstrated both the stability and the successful uptake of **10**-marked CPNPs in physiological environments, hinting at the potential of functional chain-extended catechol-based compounds (**10**) as auxiliary ligands for the design of multifunctional nanocarriers for biomedical applications.

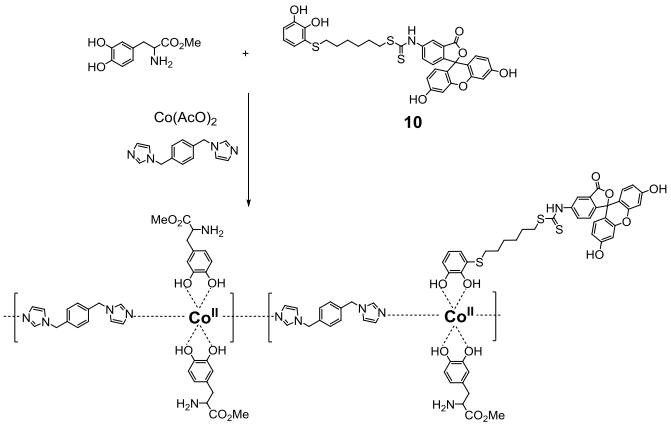

Scheme 4. Synthesis of **10**-marked fluorescent coordination polymer nanoparticles.

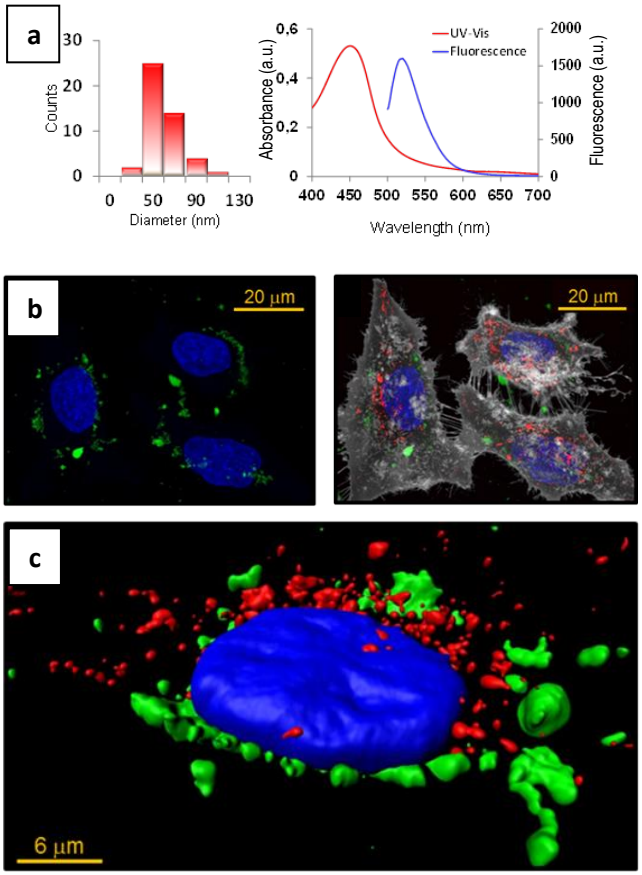

Figure 6. a) Size distribution (SEM) and fluorescence response (excitation, red line; emission, blue line) of **10**-marked CPNPs; **b)** Confocal fluorescence microscopy images of dopaminergic human neuroblastoma (BE)2-M17 cells cultured *in vivo* with **10**-marked CPNPs showing accumulated CPNPs inside cells (green). Cell membranes stained with cell mask (grey), cell nuclei with Hoechst staining (blue); and liposomes with LysoTracker® Red; **c)** 3D reconstructed image of a single cell.

Conclusions

A versatile and unified methodology to prepare functional catechol derivatives with optimal carbon atom efficiency and robust attachment of the functional moiety has been investigated by means of a conjugate addition reaction of functional thiols to freshly prepared *o*-benzoquinone from simple pyrocatechol, using a straightforward protocol. This synthetic strategy is reminiscent of mechanisms found in nature –such as the repair-and-crosslink role of thiolated moieties responsible for the restoration of the catecholic function in mussel foot proteins-, and we have shown that it may be readily co-opted to gain access to a wide scope of functional catechol derivatives incorporating aliphatic, fluorinated, PEGylated chains, or fluorescent tags, among other functional units, as well as to chain extensions. In most cases, the conjugated addition of the thiol proceeds regioselectively at the 3-position of the quinone, which was rationalized by means of theoretical DFT calculations taking into account feasible reaction pathways.

In order to showcase the potential usefulness of S-catecol compounds for surface energy modification, alkyl, fluoroalkyl and PEGylated derivatives thus prepared were successfully incorporated as coatings to tune the wettability of macroscopic surfaces and the dispersability of nanoparticles. Furthermore, a chain-extended catechol bearing a fluorescent tag was used as a ligand to build a new theranostic coordination-polymer-based nanocarrier, which showed satisfactory *in vitro* cell internalization and biomarking capabilities. Overall, the catechol derivatives reported here should be of general interest to materials chemistry, as well as for biomedical applications requiring adequate stabilization and internalization of nanostructured theranostic agents.

Experimental Section

Materials and Methods. All reagents were purchased from Sigma-Aldrich and used as received. Synthesis-grade solvents were purchased from Scharlab, S.L. and used without further purification. Opti-MEM medium, fetal bovine serum and commercial fluorescent dyes were purchased from Thermo Fischer Scientific. Human BE(2)-M17 cells were obtained from the American Type Culture Collection (ATCC). 1,4-bis(imidazol-1-ylmethyl)benzene was synthesized following a reported procedure.[21] Oleic acid-stabilized iron oxide nanoparticles were prepared according to a reported procedure.[22]

Fourier transform infrared spectroscopy (FT-IR) was carried out on a Thermo Nicolet Nexus equipped with a Goldengate attenuated total reflectance (ATR) device (neat samples), or on a Bruker Tensor 27 FT-IR spectrometer (KBr pellets). NMR spectra were recorded on Bruker DPX250, DPX360 and ARX400 spectrometers. ESI-MS was carried out in negative mode on an Agilent 6545 Q-TOF mass spectrometer. Cyclic voltammetry (CV) experiments were run on a CHI 660D Electrochemical Station (CHI Instruments), using a non-aqueous Ag/Ag^+ reference electrode containing 10 mM of $AgNO_3$, a Pt wire as counterelectrode and a glassy carbon working electrode (surface area: 4.71 mm^2). Scanning electron microscopy (SEM) and scanning transmission electron microscopy (STEM) images were acquired on a FEI Magellan 400L in extreme resolution mode (XHR) at 20 kV, using a carbon coated copper grid as support. Scanning-transmission electron microscopy (STEM) images and energy dispersive X-ray (EDX) line scan profiles were obtained at room temperature and 200 kV on a FEI Tecnai G2 F20 coupled to an EDAX detector. UV/Vis spectra were recorded on a Cary 4000 spectrophotometer (Agilent). Fluorescence emission was measured on a Hitachi F-2500 fluorescence spectrophotometer with excitation and emission slits of 5 nm and a photomultiplier tube (PMT) voltage of 400 V. Optical and fluorescence images were recorded on a Zeiss Axio Observer Z-1 inverted optical/fluorescence microscope with a motorized XY stage, Hg-lamp excitation source, AxioCam HRc digital camera, and standard filters, and in fluorescence mode with an Alexa Fluor 546 filter. Cells were imaged in vivo in a Leica TCS SP5 confocal fluorescence microscope at 37°C. Image analysis and 3D reconstruction was carried out with Bitplane Imaris software.

Geometry optimizations were carried out with the hybrid PBE0 functional[23] at the def2-TZVP level of theory.[24] In addition, the Grimme's dispersion correction[25a] was also included as implemented in Turbomole 7.0[25b]. In order to characterize the nature (minimum or transition state)

of optimized structures, the analysis of the corresponding frequencies was conducted at the same level of theory. Thus, minima are described by the absence of negative eigenvalues (imaginary frequencies, N_{imag} = 0) whereas transition states (TS) present one imaginary frequency (N_{imag} = 1) in all cases. Implicit solvent effects (CH_2Cl_2) were considered during the optimization by applying the polarizable continuum model (PCM) with the integral equation formalism variant (IEFPCM)[26] by means of a single point calculations at the same level of theory using the Gaussian 16 package.[27] Representative models were selected for each reaction as trade-offs between accuracy and computational cost. The molecular electrostatic potential (MEP) surface of *o*-benzoquinone (isosurface, 0.001 a.u.) was also computed at PBE0-D3/def2-TZVP level of theory to study differences of electrophilicity in carbon atoms. In addition, the "non-covalent interaction plot" (NCIplot) isosurfaces[28a] were also computed with the aim to confirm the additional hydrogen bonding interaction found in these structures. The colour codes (red-yellow-green-blue) of surfaces in this schematic representation are red for ρ_{cut}^{+} (repulsive) and blue for ρ_{cut}^{-} (attractive). "Atoms-in-molecules" theory[28b] has been implemented by means of the AIMall calculation package. [28c]

Syntheis of *o*-benzoquinone. To a solution of 936 mg of $NaIO_4$ (4.4 mmol) in 150 mL of H_2O cooled in an ice bath, a solution of 440 mg of pyrocatechol (4 mmol) in 5 mL of Et_2O was added and left stirring vigorously for 15 min. The orange-reddish reaction mixture was extracted with 4x15 mL of CH_2Cl_2, and the organic phase concentrated to about 1/5 of the original volume under reduced pressure. 15 mL of *n*-Hexane were added to the concentrate and the mixture cooled down to -10°C. Crystallization yielded 265 mg of pure *o*-benzoquinone (61%) as deep red needles. ^{1}H NMR (360 MHz, $CDCl_3$) *δ*: 7.05 (dd, *J* = 8.0, 3.6 Hz, 2H), 6.41 (dd, *J* = 8.0, 3.6 Hz, 2H). ^{13}C NMR (90 MHz, $CDCl_3$) *δ*: 180.5, 139.5, 131.1.

General procedure for the telescoped synthesis of functional catecholic mono-adducts (2). For the preparation **2a**-**e**, 1 mmol of the corresponding thiol (**1a-e**) was dissolved in 2 mL of CH_2Cl_2 in a Schlenk flask under nitrogen. To this, 229.5 µL of trifluoroacetic acid (TFA, 3 mmol) were added with stirring. In a separate flask, a solution of 234 mg of $NaIO_4$ (1.1 mmol) in 38 mL of H_2O was prepared and cooled in an ice bath. 110 mg of pyrocatechol (1 mmol) dissolved in 1 mL of Et_2O were added to the aqueous solution and left stirring vigorously for 15 min. The orange-reddish *o*-benzoquinone was extracted with 4x8 mL of CH_2Cl_2, and the organic phase was dried over anhydrous Na_2SO_4, filtered and immediately added to the thiol solution. The reaction mixture was stirred in the dark at room temperature under nitrogen for 6 h. After this, the solvent and the TFA were evaporated under reduced pressure and the crude was purified by column chromatography. For **2c** the same procedure was carried out at half the scale stated above for all ingredients and solvents. Yields are referred to the corresponding starting thiol, unless otherwise stated (see SI for details).

3-(octadecylthio)benzene-1,2-diol 2a and **3,6-bis(octadecylthio) benzene-1,2-diol 3a**. The reaction mixture was purified by column chromatography with 9/1 hexane/ethyl acetate, yielding 242 mg (61%) of mono-adduct **2a** and 85 mg (25%) of bis-adduct **3a**. **2a:** White solid; IR (neat): ν_{max} 3384, 2959, 2915, 2851, 1602, 1590, 1470, 1251 cm^{-1};^{1}H NMR (360 MHz, $CDCl_3$) δ: 7.00 (dd, *J* = 8.0, 1.7 Hz, 1H), 6.91 (dd, *J* = 7.8, 1.7 Hz, 1H), 6.78 (dd, *J* = 8.0, 7.8 Hz, 1H), 6.59, 5.34, (2 x br. s, 2H), 2.71 (dd, *J* = 7.9, 7.0 Hz, 2H), 1.63-1.52 (m, 2H), 1.40-1.25 (m, 30H), 0.90-0.87 (m, 3H); ^{13}C NMR (90 MHz, $CDCl_3$) δ: 143.3, 142.9, 125.7, 119.9, 118.4, 115.3, 35.9, 31.1, 28.9, 28.8, 28.8, 28.7, 28.6, 28.5, 28.3, 27.7, 21.8, 13.3; HRMS (ESI) *m/z* calculated for $C_{24}H_{42}NaO_2S$ [M + Na]$^+$: 417.2803; found 417.2785. **3a:** White solid; IR (neat): ν_{max} 3538, 3386, 2918, 2851, 1600, 1475, 1440, 1297 cm^{-1};^{1}H NMR (360 MHz, $CDCl_3$) *δ*: 6.93 (s, 2H), 6.35 (br.s, 2H), 2.76 (dd, *J* = 7.5, 7.2 Hz, 4H), 1.52-1.66 (m, 4H), 1.43-1.23 (m, 60H), 0.91-0.86- (m, 6H); ^{13}C NMR (90 MHz, $CDCl_3$) *δ*: 143.8, 124.9, 121.0, 35.7, 32.1, 29.8, 29.8, 29.7, 29.7, 29.6, 29.5, 29.3, 28.8, 22.8, 14.3; HRMS (ESI) *m/z* calculated for $C_{42}H_{79}O_2S_2$ [M + H]$^+$: 679.5521; found 679.5363.

3-((1*H*,1*H*,2*H*,2*H*-perfluorodecyl)thio)benzene-1,2-diol 2b and **3,6-bis((1*H*,1*H*,2*H*,2*H*-perfluorodecyl)thio)benzene-1,2-diol 3b**. The reaction mixture was purified by column chromatography with 7/3 hexane/ethyl acetate, yielding 218 mg (37%) of mono-adduct **2b** and 85 mg (16%) of bis-adduct **3b**. **2b:** Yellowish solid; IR (neat): ν_{max} 3447, 2959, 2924, 2854, 1608, 1587, 1488, 1464, 1342, 1240, 1208, 1146 cm^{-1};^{1}H NMR (360 MHz, $CDCl_3$) *δ*: 7.01 (dd, *J* = 7.9, 1.5 Hz, 1H), 6.97 (dd, *J* = 8.1, 1.5 Hz, 1H), 6.83 (dd, *J* = 8.1, 7.9 Hz, 1H), 2.95 (m, 2H), 2.34 (m, 2H), ArO*H* n.d.; ^{13}C NMR (90 MHz, $CDCl_3$) *δ*: 144.8, 144.6, 126.8, 125.6, 121.6, 117.4, 30.1, 27.1; elemental analysis calculated for $C_{16}H_9F_{17}O_2S$: C, 32.67; H, 1.54; S, 5.45%; found: C, 32.65; H, 1.57; S, 5.40%. **3b:** White solid; IR (neat): ν_{max} 3392, 2948, 2851, 1596, 1444, 1368, 1301, 1219, 1152 cm^{-1};^{1}H NMR (360 MHz, $CDCl_3$) *δ*: 6.98 (s, 2H), 6.26 (br.s, 2H), 3.03 (m, 4H), 2.35 (m, 4H); ^{13}C NMR (90 MHz, $CDCl_3$) *δ*:144.6, 125.7, 119.8, 110.5, 32.1, 30.1, 26.0; elemental analysis calculated for $C_{26}H_{12}F_{34}O_2S_2$: C, 29.28; H, 1.13; S, 6.01%; found: C, 29.49; H, 1.15; S, 6.15%.

3-(methoxy(polyethyleneoxy)ethylthio)benzene-1,2-diol 2c. The reaction mixture was purified by column chromatography with 8/2 to 5/5 gradient of hexane/ethyl acetate, yielding 286 mg (56%) of mono-adduct **2c**. Pale yellow oil; IR (neat): ν_{max} 3384, 2959, 2915, 2851, 1602, 1590, 1470, 1251 cm^{-1};^{1}H NMR (400 MHz, $CDCl_3$) *δ*: 6.93 (dd, *J* = 7.8, 1.5 Hz, 1H), 6.89 (dd, *J* = 8.0, 1.5 Hz, 1H), 6.66 (dd, *J* = 8.0, 7.8 Hz, 1H), 3.65-3.55 (m, >70H), 3.33 (s, 3H), 2.92 (t, *J* = 5.8 Hz, 2H), 2.90 (t, *J* = 5.8 Hz, 2H), ArO*H* n.d.; ^{13}C NMR (100 MHz, $CDCl_3$) *δ*: 145.8, 145.2, 126.5, 120.5, 119.1, 116.7, 70.5, 69.1, 59.2, 36.0; HRMS (ESI) *m/z* calculated for $C_{47}H_{92}NO_{22}S$ [M + NH_4]$^+$ 1054.5832; found 1054.5826; HRMS (MALDI) *m/z* calculated for $C_{47}H_{88}NaO_{22}S$ [M + Na]$^+$ 1059.5386; found 1059.5522, both corresponding to n = 19, together with several satellite peaks corresponding to n around 20.

4-(benzo[d]thiazol-2-ylthio)benzene-1,2-diol 2d. The reaction mixture was purified by column chromatography with 7/3 hexane/ethyl acetate, yielding 175 mg (64%) of mono-adduct **1d**. Orange solid; IR (neat): ν_{max} 3517, 3433, 3053, 2927, 2687, 2544, 1595, 1504, 1451, 1416, 1320, 1276, 1028 cm^{-1};^{1}H NMR (360 MHz, CD_3OD) *δ*: 7.76 (d, *J* = 7.5 Hz, 1H), 7.73 (d, *J* = 7.4 Hz, 1H), 7.42 (dd, *J* = 7.7, 7.5 Hz, 1H), 7.28 (dd, *J* = 7.7, 7.4 Hz, 1H) 7.17 (d, *J* = 2.1 Hz, 1H), 7.11 (dd, *J* = 8.1, 2.1 Hz, 1H), 6.93 (d, *J* = 8.1 Hz, 1H); ^{13}C NMR (90 MHz, CD_3OD) *δ*: 143.3, 142.9, 125.7, 119.9, 118.4, 115.3, 35.9, 31.1, 28.9, 28.8, 28.8, 28.7, 28.6, 28.5, 28.3, 27.7, 21.8, 13.3; HRMS (ESI) *m/z* calculated for $C_{13}H_9NNaO_2S_2$ [M + Na]$^+$ 297.9972; found 297.9963.

7-((2,3-dihydroxyphenyl)thio)-4-methyl-2H-chromen-2-one 2e. The reaction mixture was purified by column chromatography with 1/1 hexane/ethyl acetate, yielding 67 mg (45%) of mono-adduct **2e**. Brownish solid; IR (neat): ν_{max} 3421, 3251, 2956, 2913, 2597, 2422, 1707, 1675, 1599, 1584, 1537, 1473 cm^{-1};^{1}H NMR (360 MHz, $(CD_3)_2SO$) *δ*: 9.83 (br. s, 1H), 9.14 (br. s, 1H), 7.68 (d, *J* = 8.2, 1.6 Hz, 1H), 7.08 (d, *J* = 8.2 Hz, 1H), 6.99 (dd, *J* = 7.9, 1.5 Hz, 1H), 6.91 (dd, *J* = 7.8, 1.5 Hz, 1H), 6.89 (d, *J* = 1.6 Hz, 1H), 6.78 (dd, *J* = 7.9, 7.8 Hz, 1H), 6.33 (s, 1H), 2.41 (s, 3H); ^{13}C NMR (90 MHz, $(CD_3)_2SO$) *δ*: 160.8, 154.4, 153.7, 146.3, 144.0, 126.9, 126.5, 122.8, 120.8, 117.9, 117.4, 115.8, 113.4, 113.1, 18.7; elemental analysis calculated for $C_{16}H_{12}O_4S$: C, 63.99; H, 4.03; S, 10.68%; found: C, 64.03; H, 4.01; S, 10.62%.

Synthesis of chain-extended catechol-thiols (5) and bis-catechols (6).

Method A: by direct reaction between *o*-benzoquinone and a dithiol (**4**) The general procedure for the conjugate addition was followed, by employing 0.5 mmol or 1 mmol of dithiol (**4a**-**d**). Crudes were purified by column chromatography. Yields are referred to the corresponding starting dithiol (**4**), unless otherwise stated (see SI for details).

Method B: selective synthesis of catechol-thiols (**5**) from dithiols (**4**), including protection/deprotection steps **Synthesis of monoacetylated dithiols (7)**. 3 mmol of dithiol (**4b** and **4c**) were dissolved in 17 mL of CH_2Cl_2. To this, 17 mL of pyridine and 282 µL of acetic anhydride (2.5 mmol) were added and stirred at room temperature for 16 hours. The solvent was removed under reduced pressure, and the residue repeatedly extracted with distilled water in order to remove the pyridine completely, dried and evaporated under reduced pressure. Analysis of the ^{1}H-NMR spectra of the washed crudes showed that **7b** and **7c** were obtained approximately in 65% and 71% yields, respectively, mixed their respective diacetylation side-products, as well as with very low amounts (≤5% and ≤2%, respectively) of unreacted dithiols. Since the diacetylated compounds do not participate in the subsequent conjugate addition and the starting dithiols were present in residual amounts, these crudes were used in the next step without further purification. **Synthesis of catechol thioacetates (8)**. The general procedure for the conjugate addition was followed, by using aliquots of the reaction crudes containing ca. 1 mmol of the corresponding monoacetylated dithiol **7b or 7c** (295 mg of crude **7b** and 315 mg of crude **7c** for respective purities of 65% and 71%, according to the 1H-NMR spectrum). Crudes were purified by column chromatography with 7/3 hexane/ethyl acetate, yielding of 133 mg (45%) of **8b** and 138 mg (44%) of **8c**. **Synthesis of catechol-thiols (5)**. To a solution of 150 mg of **8b** or 166 mg of **8c** in 10 mL of MeOH, 100 µL of concentrated HCl (37%) were added. The mixture was refluxed with stirring for 15 h. After this, the solvent was removed under reduced pressure, 5 mL of distilled water were added and the organic fraction was extracted with ethyl acetate (3x3 mL), dried over anhydrous Na_2SO_4 and filtered. The solvent was finally evaporated under reduced pressure, yielding 126 mg (98%) of **5b** or 142 mg (98%) of **5c**.

3-((3-mercaptobuyl)thio)benzene-1,2-diol 5a and **3,3'-(butane-1,3-diylbis(sulfanediyl))bis(benzene-1,2-diol) 6a**. Using Method A, the reaction mixture was purified by column chromatography with 8/2 of hexane/ethyl acetate, yielding 76 mg (33%) of catechol-thiol **5a**, and 37 mg (11%) of bis-catechol **6a**. **5a:** Pale yellow oil; IR (neat): ν_{max} 3450, 2928, 2901, 2540, 1584, 1453, 1326, 1198, 902 cm^{-1};^{1}H NMR (360 MHz, $CDCl_3$) *δ*: 6.99 (dd, *J* = 7.7, 1.3 Hz, 1H), 6.91 (dd, *J* = 8.0, 1.3 Hz, 1H), 6.77 (deform dd, *J* = 8.0, 7.7 Hz, 1H), 6.64, 5.83 (2xbr.s, 2H), 2.74-2.63 (m, 2H), 2.54-2.44 (m, 2H), 1.76-1.58 (m, 4H), 1.34 (t, *J* = 7.8, 1H); ^{13}C NMR (90 MHz, $CDCl_3$) *δ*: 144.4, 144.0, 126.7, 121.0, 119.3, 116.6, 36.0, 32.9, 28.4, 24.3; elemental analysis calculated for $C_{10}H_{14}O_2S_2$: C, 52.14; H, 6.13; S, 27.84%; found: C, 52.12; H, 6.10; S, 27.79%. **6a:** Pale orange oil; IR (neat): ν_{max} 3460, 2931, 2545, 1578, 1339, 1201 cm^{-1}; ^{1}H NMR (400 MHz, $CDCl_3$) δ: 6.96 (dd, *J* = 7.7, 1.5 Hz, 2H), 6.91 (dd, *J* = 8.1, 1.5 Hz, 2H), 6.78 (dd, *J* = 8.1, 7.7 Hz, 2H), 2.75-2.60 (m, 4H), 1.72-1.54 (m, 4H); ^{13}C NMR (100 MHz, $CDCl_3$) δ: 144.5, 144.2, 126.9, 121.2, 119.1, 116.8, 36.3, 28.8; elemental analysis calculated for $C_{16}H_{18}O_4S_2$: C, 56.78; H, 5.36; S, 18.95%; found: C, 56.83; H, 5.31; S, 18.99%.

3-((6-mercaptohexyl)thio)benzene-1,2-diol 5b and **3,3'-(hexane-1,6-diylbis(sulfanediyl))bis(benzene-1,2-diol) 6b**. Using Method A, the reaction mixture was purified by column chromatography with 8/2 of hexane/ethyl acetate, yielding 90 mg (35%) of catechol-thiol **5b**, and 132 mg (36%) of bis-catechol **6b**. Using Method B, the overall yield of **5b** is 43%. **5b:** Pale yellow oil; IR (neat): ν_{max} 3467, 3187, 2930, 2854, 2545, 1614, 1584, 1459, 1327, 1219, 898 cm−1;^{1}H NMR (400 MHz, $CDCl_3$) δ: 6.99 (dd, *J* = 7.8, 1.5 Hz, 1H), 6.92 (dd, *J* = 8.0, 1.5 Hz, 1H), 6.79 (dd, *J* = 8.0, 7.8 Hz, 1H), 6.57, 5.35 (2xbr.s, 2H), 2.71 (dd, *J* =7.5, 7.3 Hz, 2H), 2.50 (ddd, *J* = 7.5, 7.3, 7.3 Hz, 2H), 1.62-1.51 (m, 4H), 1.44-1.35 (m, 4H), 1.33 (t, *J* = 7.5, 1H); ^{13}C NMR (100 MHz, $CDCl_3$) δ: 144.4, 144.1, 126.9, 121.0, 119.4, 116.6, 36.8, 34.0, 29.8, 28.3, 28.1, 24.8; HRMS (ESI) *m/z* calculated for $C_{12}H_{19}O_2S_2$ $[M + H]^+$: 259.0826; found 259.0678. **6b:** Pale yellow oil; IR (neat): ν_{max} 3458, 3180, 2926, 2546, 1570, 1390, 1190 cm^{-1}; ^{1}H NMR (400 MHz, $CDCl_3$) δ: 6.98 (dd, *J* = 7.8, 1.6 Hz, 2H), 6.90 (dd, *J* = 8.0, 1.6 Hz, 2H), 6.77 (dd, *J* = 8.0, 7.8 Hz, 2H), 4.92 (br.s, 4H), 2.68 (t, *J* = 7.3, 4H), 1.55-1.51 (m, 4H), 1.40-1.33 (m, 4H); ^{13}C NMR (100 MHz, $CDCl_3$) δ: 144.5, 144.2, 126.8, 121.0, 119.2, 116.7, 36.8, 29.7, 28.3; elemental analysis calculated for $C_{18}H_{22}O_4S_2$: C, 58.99; H, 6.05; S, 17.50%; found: C, 59.01; H, 6.04; S, 17.52%.

3-((2-(2-(2-mercaptoethoxy)ethoxy)ethyl)thio)benzene-1,2-diol 5c and **3,3'-(((ethane-1,2-diylbis(oxy))bis(ethane-2,1-diyl))bis(sulfanediyl))bis(benzene-1,2-diol) 6c**. Using Method A, the reaction mixture was purified by column chromatography with 7/3 of hexane/ethyl acetate, yielding 102 mg (35%) of catechol-thiol **5c**, and 44 mg (11%) of bis-catechol **6c**. Using Method B, the overall yield of **5c** is 41%. **5c:** Pale orange oil; IR (neat): ν_{max} 3460, 3175, 2925, 2500, 1732, 1625, 1580, 1315, 1201, 903 cm^{-1};^{1}H NMR (400 MHz, $CDCl_3$) *δ*: 7.59 (br. s, 1H), 6.99 (dd, *J* = 7.8, 1.5 Hz, 1H), 6.92 (dd, *J* = 8.0, 1.5 Hz, 1H), 6.73 (dd, *J* = 8.0, 7.8 Hz, 1H), 5.79 (br. s, 1H), 3.69-3.66 (m, 4H), 3.64 (t, *J* = 6.4 Hz, 2H), 3.56 (t, *J* = 5.8 Hz, 2H), 2.92 (t, *J* = 5.8 Hz, 2H), 2.72 (dt, *J* = 8.2, 6.4 Hz, 2H), 1.65 (t, *J* = 8.2 Hz, 1H); ^{13}C NMR (100 MHz, $CDCl_3$) *δ*: 145.7, 144.9, 127.6, 120.9, 118.7, 116.8, 73.2, 70.4, 70.2, 69.0, 36.9, 24.6; HRMS (ESI) *m/z* calculated for $C_{12}H_{19}O_4S_2$ $[M + H]^+$: 291.0725; found 291.0607. **6c:** Pale yellow oil; IR (neat): ν_{max} 3445, 2935, 2510, 1617, 1548, 1196 cm^{-1};^{1}H NMR (400 MHz, $CDCl_3$) *δ*: 7.65 (br.s, 2H), 7.01 (dd, *J* = 7.8, 1.5 Hz, 2H), 6.93 (dd, *J* = 8.0, 1.5 Hz, 2H), 6.76 (dd, *J* = 8.0, 7.8 Hz, 2H), 5.85 (br.s, 2H), 3.70 (s, 4H), 3.57 (t, J = 5.8 Hz, 2H), 2.94 (t, J = 5.8 Hz, 2H); ^{13}C NMR (100 MHz, $CDCl_3$) *δ*: 145.8, 144.9, 127.8, 121.0, 118.7, 117.0, 70.2, 69.0, 37.0; elemental analysis calculated for $C_{18}H_{22}O_6S_2$: C, 54.25; H, 5.56; S, 16.09%; found: C, 54.23; H, 5.53; S, 16.02%.

3-(((2*R,3*R**)-2,3-dihydroxy-4-mercaptobutyl)thio)benzene-1,2-diol 5d.** Using Method A, the reaction mixture was purified by column chromatography with 6/4 to 4/6 gradient of hexane/ethyl acetate, yielding 87 mg (33%) of catechol-thiol **5d**. Pale yellow oil; IR (neat): ν_{max} 3510, 3412, 2925, 2901, 1325, 1230, 1181cm^{-1}; ^{1}H NMR (400 MHz, CD_3OD) *δ*: 6.90 (dd, *J* = 7.7, 1.6 Hz, 1H), 6.74 (dd, *J* = 7.9, 1.6 Hz, 1H), 6.64 (dd, *J* = 7.9, 7.7 Hz, 1H), 3.71 (ddd, *J* = 7.6, 5.5, 2.7 Hz, 1H), 3.66 (dt, *J* = 6.5, 2.7 Hz, 1H), 3.03 (dd, *J* = 13.4, 5.5 Hz, 1H), 2.91 (dd, *J* = 13.4, 7.6 Hz, 1H), 2.61 (d, *J* = 6.5 Hz, 2H); ^{13}C NMR (100 MHz, CD_3OD) *δ*: 146.6, 146.4, 125.7, 121.7, 120.8, 116.3, 75.2, 71.6, 38.9, 28.2; elemental analysis calculated for $C_{10}H_{14}O_4S_2$: C, 45.78; H, 5.38; S, 24.44%; found: C, 45.81; H, 5.33; S, 24.46%.

S-(6-mercaptohexyl)ethanethioate 7b. Yellowish oil; IR (neat): ν_{max}, 2965, 2930, 2860, 1715, 1325, 1235, 899 cm^{-1}; ^{1}H NMR (360 MHz, $CDCl_3$) *δ*: 2.84 (t, *J*= 7.3 Hz, 2H), 2.50 (ddd, *J* = 7.7, 7.4, 7.3 Hz, 2H), 2.30 (s, 3H), 1.63-1.51 (m, 4H),1.42-1.34 (m, 4H), 1.31 (t, *J*= 7.7 Hz, 1H); ^{13}C NMR (90 MHz, $CDCl_3$) *δ*: 196.2, 39.2, 34.1, 30.9, 29.7, 29.3, 28.6, 24.8.

S-(2-(2-(2-mercaptoethoxy)ethoxy)ethyl)ethanethioate 7c. Yellowish oil; IR (neat): ν_{max}, 2890, 2562, 1695, 1520, 1420, 1325, 1191, 888 cm^{-1}; ^{1}H NMR (360 MHz, $CDCl_3$) *δ*: 3.66-3.55 (m, 6H), 3.06 (t, *J*= 6.5 Hz, 2H), 2.67 (ddd, *J* = 8.2, 6.5, 6.4 Hz, 2H), 2.31 (s, 3H), 1.57 (t, *J*= 8.2 Hz, 1H); ^{13}C NMR (90 MHz, $CDCl_3$) *δ*: 195.7, 73.2, 70.5, 70.4, 70.0, 30.8, 29.1, 24.5.

S-(6-((2,3-dihydroxyphenyl)thio)hexyl)ethanethioate 8b. After step 2 of Method B, the reaction mixture was purified by column chromatography with 7/3 hexane/ethyl acetate, yielding 133 mg (44%) of

8b. Pale yellow oil; IR (neat): ν_{max} 3420, 3155, 2930, 2540, 2425, 1709, 1190 cm^{-1}; ^1H NMR (360 MHz, $CDCl_3$) δ: 6.98 (dd, *J* = 7.8, 1.3 Hz, 1H), 6.90 (dd, *J* = 8.1, 1.3 Hz, 1H), 6.77 (dd, *J*= 8.1, 7.8 Hz, 1H), 6.58 (br. s, 1H), 5.61 (br. s, 1H), 2.84 (t, *J*= 7.3 Hz, 2H), 2.70 (t, *J* = 7.3 Hz, 2H), 2.32 (s, 3H), 1.60-1.50 (m, 4H), 1.45-1.30 (m, 4H); ^{13}C NMR (90 MHz, $CDCl_3$) δ: 196.5, 144.5, 144.1, 126.8, 121.0, 119.5, 116.5, 39.2, 36.7, 35.5, 30.9, 29.7, 29.2, 28.4; HRMS (ESI) *m/z* calculated for $C_{14}H_{21}O_3S_2$ $[M + H]^+$: 301.0932; found 301.0678.

S-(2-(2-(2-((2,3-dihydroxyphenyl)thio)ethoxy)ethoxy)ethyl) ethanethioate 8c. After step 2 of Method B, the reaction mixture was purified by column chromatography with 7/3 hexane/ethyl acetate, yielding 138 mg (42%) of **8c**. Pale yellow oil; IR (neat): ν_{max} 3433, 2927, 2899, 2430, 1705, 1325, 1196 cm^{-1}; ^1H NMR (360 MHz, $CDCl_3$) δ: 7.60 (br. s, 1H), 6.99 (dd, *J* = 7.8, 1.5 Hz, 1H), 6.91 (dd, *J* = 8.0, 1.5 Hz, 1H), 6.73 (dd, *J* = 8.0, 7.8 Hz, 1H), 5.89 (br. s, 1H), 3.68-3.64 (m, 4H), 3.61 (t, *J* = 6.7 Hz, 2H), 3.55 (t, *J* = 5.7 Hz, 2H), 3.11 (t, *J* = 6.7 Hz, 2H), 2.91 (t, *J* = 5.7 Hz, 2H), 2.33 (s, 3H); ^{13}C NMR (90 MHz, $CDCl_3$) δ: 196.1, 145.8, 144.9, 127.6, 120.7, 118.8, 116.7, 70.4, 70.2, 70.1, 69.0, 36.9, 30.9, 29.0; HRMS (ESI) *m/z* calculated for $C_{14}H_{21}O_5S_2$ $[M + H]^+$: 333.0830; found 333.0713.

Synthesis of 3,3'-[disulfanediylbis(hexane-2,1-diylsulfanediyl)] dibenzene-1,2-diol 9. To a solution of 55 mg of **5b** (0.213 mmol) in 1.5 mL of CH_2Cl_2, a solution of 54 mg of I_2 (0.213 mmol) in 2 mL of CH_2Cl_2 was added dropwise. The reaction mixture was stirred at room temperature for 20 min, and extracted with a 10% sodium thiosulfate solution in water. The organic phase was separated and dried over Na_2SO_4, obtaining disulfide **9** as an orange oil in quantitative yield. IR (neat): ν_{max} 3386, 2926, 2853, 1591, 1455, 1330, 1245, 1221, 1136, 1058, 895 cm^{-1}; ^1H NMR (360 MHz, $CDCl_3$) δ: 7.00 (dd, *J* = 7.8, 1.5 Hz, 2H), 6.93 (dd, *J* = 8.0, 1.5 Hz, 2H), 6.80 (dd, *J* = 8.0, 7.8 Hz, 2H), 6.58, 5.39 (2xbr.s, 4H), 2.72 (t, *J* =7.5 Hz, 4H), 2.67 (t, *J* = 7.5 Hz, 4H), 1.67 (m, 8H), 1.40 (broad m, 8H); ^{13}C NMR (90 MHz, $CDCl_3$) δ: 144.2, 143.8, 126.6, 120.8, 119.1, 116.3, 38.8, 36.6, 29.5, 28.9, 28.1, 27.9 HRMS (ESI) *m/z* calculated for $C_{18}H_{22}NaO_4S_2$ $[M + Na]^+$: 389.0857; found 389.1238.

Synthesis of 6-((2,3-dihydroxyphenyl)thio)hexyl(3,6-dihydroxy-3'-oxo-3'H,10H-spiro[anthracene-9,1'-isobenzofuran]-5'-yl) carbamodithioate 10. To a solution of 55 mg of **5b** (0.21 mmol) in 4 mL of acetone, 83 mg of fluorescein isothiocyanate (0.21 mmol) were added, and the reaction mixture refluxed under magnetic stirring for 24 h. The solvent was then removed under reduced pressure, and the residue purified by column chromatography with 6/4 hexane/ethyl acetate, yielding 83 mg (60%) of **10** as a dark orange solid (λ_{ex} = 450 nm, λ_{em} = 520 nm). IR (neat): ν_{max} 3552, 3490, 3325, 3182, 2920, 2899, 2535, 1725, 1695, 1565, 1455, 1390, 1173 cm^{-1}; ^1H NMR (360 MHz, $(CD_3)_2CO$) δ: 10.9 (br.s, 1H), 8.90 (br.s, 1H), 8.58 (s, 1H), 8.11 (dd, dd, *J* = 8.3, 2.0 Hz, 1H), 7.30 (dd, *J* = 8.3, 0.5 Hz, 1H), 6.86 (dd, *J* = 7.8, 1.6 Hz, 1H), 6.78 (dd, *J* = 8.0, 1.6 Hz, 1H), 6.76 (s, 2H), 6.75-6.70 (m, 2H), 6.71 (s, 2H), 6.66 (dd, *J*= 8.0, 7.8 Hz, 1H), 6.64 (d, *J*= 8.7 Hz, 1H), 3.32 (dd, *J* = 7.5, 7.2 Hz, 2H), 2.84 (t, *J* = 7.2 Hz, 2H), 1.72 (p, *J* = 7.3 Hz, 2H), 1.60 (p, *J* = 7.4 Hz, 2H), 1.53-1.39 (m, 4H), Catechol-O*H* nd; ^{13}C NMR (90 MHz, $(CD_3)_2CO$) δ: 199.1, 160.3, 153.3, 150.7, 145.7, 145.6, 142.2, 131.2, 130.1, 128.3, 125.2, 124.1, 122.2, 120.6, 119.1, 115.4, 113.3, 111.4, 103.3, 35.7, 34.3, 30.6, 29.9, 29.5, 29.0, 28.8; HRMS (ESI) *m/z* calculated for $C_{33}H_{30}NO_7S_3$ $[M + H]^+$: 648.1184; found 648.1162.

Cyclic voltammetry. Prior to the experimental runs, a 50 mM stock solution of tetrabutylammonium hexafluorophosphate ($TBAPF_6$) in CH_2Cl_2 previously dried over molecular sieves (4 Å) was used to prepare the test medium, as well as to set up the non-aqueous Ag/Ag+ (10 mM $AgNO_3$) reference electrode. For each experiment, 9 mL of the stock electrolyte solution were mixed with 0.5 mL of a 0.3 M solution of trifluoroacetic acid in CH_2Cl_2, purged with nitrogen (5') and a baseline recorded. After further purging (5'), 0.5 mL of a 0.1 M solution of the analyte (pyrocatechol, octadecanethiol **1a**, or 3-octadecylthiocatechol **2a**) in CH_2Cl_2 were added, and the CV was recorded. Baselines and experimental runs consisted of two consecutive oxidation/reduction cycles between -0.1 V and 2 V vs non-aqueous Ag/Ag^+, at a 100 mV/s sweep rate. Prior to each experiment, the glassy carbon working electrode was polished on sandpaper (1200 grit), followed by with 1 μm and 0.3 μm alumina slurry on Nylon cloth.

Oxidative polymerization of mono-adducts (2) in ammonia/air. Following a previously reported procedure,[5] 0.394 g of **2a** or 0.588 g of **2b** (1 mmol) were dissolved in 70 mL of isopropanol, to which 7.55 mL of NH_3 aq., 25%, 100 mmol) were added. The mixture was stirred at 55°C for 6 hours. After this, 60 mL of H_2O were added, the organic solvent was evaporated under reduced pressure, and the crude was brought to pH~5 by dropwise addition of concentrated HCl (37%). The mixture was extracted with an appropriate solvent (CH_2Cl_2 or THF, 3 x 20 mL), dried over anhydrous $NaSO_4$, and the solvent removed under reduced pressure, yielding 0.350 g (89%) of **p2a** (thick, black oil) or 0.505 mg (86%) of **p2b** (black solid).

Dip-coating of macroscopic substrates. A rectangular surface (TiO_2 or cotton cloth) of approx. 4 cm^2 was immersed for 3 h in a 10mM solution of a mono-adduct (**2a**, **2b**), bis-adduct (**3a**, **3b**) or ammonia-polymerized (**p2a**, **p2b**) catechol derivative in an appropriate solvent (**2a**, **p2a** and **3a** in CH_2Cl_2, **2b**, **p2b** and **3b** in THF). The substrate was then washed thoroughly with MeOH and dried under a N_2 flow. For cotton cloth, a piece of about 4 cm^2 was immersed for 2 min in a 1% (w/v) solution of **p2a** in *n*-hexane or **p2b** in THF, rinsed, washed thoroughly with MeOH and dried under a N_2 flow.

Coating of mesoporous silica nanoparticles (MSNs). To a solution of 51.4 mg of **9** (0.1 mmol) in 13 mL of isopropanol, 5 mg of MSNs (Ø ~ 250 nm) and 0.75 mL of 25% wt aqueous ammonia (10 mmol) were added. The suspension was stirred at 200 rpm and 45°C for 16 h, centrifuged (7500 rpm, 5 min) and washed successively with 1x3 mL of water and 2x3 mL of EtOH.

Coating of magnetite nanoparticles. 300 μL of a suspension of oleic-acid stabilized iron oxide (Fe_xO_y) nanoparticles in *n*-hexane (ca. 20 mg/mL) was added to a solution of 15 mg of **2c** (0.017 mmol) in 1 mL CH_2Cl_2, and stirred for 15 hours. After this, the sample was centrifuged, washing once with CH_2Cl_2 and 4 times with *n*-hexane. Iron oxide NPs were then re-suspended in a water/*n*-hexane mixture and shaken, where they were shown to extract to the aqueous layer.

Synthesis of theranostic CPPs with 10 as fluorescent ligand. A mixture of 48 mg (0.195 mmol) of L-DOPA methyl ester hydrochloride, 3 mg (0.0046 mmol) of **10** and 24 mg (0.1 mmol) of 1,4-bis(imidazol-1-ylmethyl)benzene (BIX) were dissolved in 12 mL of EtOH. Under magnetic stirring (1000 rpm), an aqueous solution of 25 mg (0.10 mmol) of $Co(AcO)_2{\cdot}4H_2O$ in 1.6 mL of water was added to the alcoholic solution. A brown suspension was rapidly formed, which was stirred at room temperature for 2 h. After incubation, the suspended solid was recovered by centrifugation at 8000 rpm for 10 min, the resultant pellet was re-suspended in EtOH (12 mL) and washed several times, until no free L-DOPA methyl ester or **10** were detected by fluorescence in the supernatant. The final pellet containing fluorescent coordination polymer nanoparticles was re-suspended in 1.5 mL EtOH and stored in solution at 4°C. For fluorescence measurements, samples were re-suspended in water and fluorescence emission registered between 400 and 700 nm (λ_{ex} = 450 nm).

Cell culture and cellular uptake of fluorescent CPNPs. Human BE(2)-M17 cells were maintained in Opti-MEM medium further supplemented with 10 % (v/v) of heat-inactivated fetal bovine serum (FBS). Cells were grown under a highly humidified atmosphere of 95 % air with 5 % CO_2 at 37 °C. Cellular uptake of the nanoparticles was monitored by using *in* laser scanning confocal microscopy (LSCM). For *in vitro* imaging, BE(2)-M17 cells were seeded in a 35 mm glass-bottom culture dishes at a density of $1.0x10^5$ cells per dish. After 24 h incubation the media was removed and cells were treated with control medium or with 50 µg/mL of fluorescent CPPs for 6 h at 37 °C. Simultaneously to the nanoparticles, Lyso Tracker® Red at a final concentration of 75 nM was added to the cells. Immediately before imaging, cells were washed three times with 1 mL of fresh medium, and then nuclei and membranes were stained with 5 µg/mL Hoechst (Invitrogen) and 1X Cell Mask for 10 min at 37 °C. Cells were imaged *in vitro* at 37 °C.

Conflict of interest

The authors declare no conflict of interest.

Acknowledgements

C.C. and M.A.M.-V. are grateful to the Spanish Ministry of Science for their pre-doctoral grants (FPU-2015-03245 and FPI-SEV-2013-0295-16-1). F.N. is grateful to the Universidad Nacional del Sur for a postdoctoral grant. This project had financial support from the Spanish Ministry of Science and EU FEDER funds (CTQ2016-75363-R and MAT2015-70615-R). We thank Prof. Antonio Frontera (Universitat de les Illes Balears) for the use of computational facilities and assistance in calculations.

Keywords: catechol chemistry • bioinspired materials • thiol conjugate addition • functional coatings • surface wetting • coordination polymers • theranostics

[1] a) J. H. Waite, M. L. Tanzer, *Science* **1981**, *212*, 1038-1040; b) J. H. Waite, X.X. Qin, *Biochemistry* **2001**, *40*, 2887-2893.; c) L. A. Burzio, J. H. Waite, *Biochemistry* **2000**, *39*, 11147-11153; d) M. J. Sever, J. T. Weisser, J. Monahan, S. Srinivasan, J. J. Wilker, *Angew. Chem. Int. Ed.* **2004**, *43*, 448-;450 e) M. Yu, J. Hwang, T. J. Deming, *J. Am. Chem. Soc.* **1999**, *121*, 5825-5826; f) V. V. Papov, T. V. Diamond, K. Biemann, J. H. Waite, *J. Biol. Chem.* **1995**, *270*, 20183-20192.;g) J. Saiz-Poseu, J. Mancebo-Aracil, F. Nador, F. Busqué, D. Ruiz-Molina, *Angew. Chem. Int. Ed.* **2019**, *58*, 696-714.

[2] a) M. Yu , T. J. Deming, *Macromolecules* **1998**, *31*, 4739-4745; b) B. P. Lee, C.-Y. Chao, F. N. Nunalee, E. Motan, K. R. Shull, P. B. Messersmith, *Macromolecules* **2006**, *39*, 1740-1748; c) S. A. Burke, M. Ritter-Jones, B. P. Lee, P. B. Messersmith, *Biomed. Mater.* **2007**, *2*, 203-210; d) G. Westwood, T. N. Horton, J. J. Wilker*, Macromolecules,* **2007***, 40*, 3960-3964.

[3] a) S. Saxer, C. Portmann, S. Tosatti, K. Gademann, S. Zürcher, M. Textor, *Macromolecules* **2010**, *43*, 1050-1060; b) H. Han, J. Wu, C. W. Avery, M. Mizutani, X. Jiang, M. Kamaigaito, Z. Chen, C. Xi, R. Lu, Y. Kamiya, T. Miyakoshi, *Talanta* **2006**, *70*, 370-376; c) B. Malisova, S. Tosatti, M. Textor, K. Gademann, S. Zürcher, *Langmuir* **2010**, *26*, 4018-4026; d) J. L. Dalsin, L. Lin, S. Tosatti, J. Vörös, M. Textor, P. B. Messersmith, *Langmuir* **2005**, *21*, 640-646; e) J. L. Dalsin, B.-H. Hu, B. P. Lee, P. B. Messersmith, *J. Am. Chem. Soc.* **2003**, *125*, 4253-4258.

[4] H. Lee, S. M. Dellatore, W. M. Miller, P. B. Messersmith, *Science* **2007**, *318*, 426-430.

[5] a) J. Sedó, J. Saiz-Poseu, F. Busqué, D. Ruiz-Molina, *Adv. Mater.* **2013**, *25*, 653-701; b) B. García, J. Saiz-Poseu, R. Gras-Charles, J. Hernando, R. Alibés, F. Novio, J. Sedó, F. Busqué, D. Ruiz-Molina, *ACS Appl. Mater. Interfaces* **2014**, *6*, 17616-17625;

[6] a) J. Saiz-Poseu, J. Sedó, B. García, C. Benaiges, T. Parella, R. Alibés, J. Hernando, F. Busqué, D. Ruiz-Molina, *Adv. Mater.* **2013**, *25*, 2066-2070; b) J. Kumanotani, *Prog. Org. Coat.* **1999**, *26*, 163; c) M. A. ElSohly, P. D. Adawadkar, C. Ma, C. E. Turner, *J. Nat. Prod.* **1982**, *45*, 532-538; d) N. N Adarsh, F. Novio, D. Ruiz-Molina, *Dalton Trans*., **2016**, *45*, 11233-11255.

[7] a) I. Y. Chukicheva, I. V. Timusheva, L. V. Spirikhin, A. V. Kuchin, *Chem. Nat. Compd.* **2007**, *43*, 245-249; b) E. Findik, M. Ceylan, M. Elmastas, *Eur. J. Med. Chem.* **2011**, *46*, 4618-4624; c) J. Duan, W. Wu, Z. Wei, D. Zhu, J. Tu, A. Zhang, *Green Chem.* **2018**, *20*, 912-920.

[8] Y. Kuninobu, T. Matsuki, K. Takai, *J. Am. Chem. Soc.* **2009**, *131*, 9914-9915.

[9] X. Liu, Y. Ou, S. Chen, X. Lu, H. Cheng, X. Jia, D. Wang, G.-C. Zhou, *Eur. J. Med. Chem.* **2010**, *45*, 2147-2153.

[10] H. Naeimi, L. Moradi, *J. Mol. Cat. A: Chem.* **2006**, *256*, 242-246.

[11] J. Yu, W. Wei, E. Danner, R. K. Ashley, J. N. Israelachvili, J. H. Waite, *Nat. Chem. Biol.* **2011**, 7, 588-590.

[12] a) K. Cao, D. E. Stack, R. Ramanathan, M. L. Gross, E. G. Rogan, E. L. Cavalieri, *Chem. Res. Toxicol.* **1998**, *11*, 909-916; b) R. Micillo, L. Panzella, K. Koike, G. Monfrecola, A. Napolitano, M. d' Ischia, *International Journal of Molecular Sciences* **2016***, 17*, 746-758.

[13] a) K. S. Feldman, A. Sambandam, K. E. Bowers, H. M. Appel, *J. Org. Chem.* **1999**, *64*, 5794-5803; b) J. S. Mitchell, Y. Wu, C. J. Cook, L. Main, *Bioconjugate Chem.* **2007**, *18*, 268-274; c) L. A. Miller, M. A. Marsini, T. R. R. Pettus, *Org. Lett.* **2009**, *11*, 1955-1958; d) T. Masuda, M. Inai, Y. Miura, A. Masuda, S. Yamauchi, *J. Agric. Food Chem.* **2013**, *61*, 1097-1104; e) A. Kotronoulas, N. Pizarro, A. Serra, P. Robledo, J. Joglar, L. Rubio, A. Hernaéz, C. Tormos, M. J. Motilva, M. Fitó, M.-I. Covas, R. Solà, M. Farré, G. Saez, R. de la Torre, *Pharmacol. Res.* **2013**, *77*, 47-56; f) Y. S. Cheah, S. Santhanakrishnan, M. B. Sullivan, K. G. Neoh, C. L. L. Chai, *Tetrahedron* **2016**, *72*, 6543-6550.

[14] a) B. V. Varun, K, R. Prabhu, *J. Org. Chem.* **2014**, *79*, 9655-9668; b) H. T. Abdel-Mohsen, J. Conrad U. Beifuss, *Green Chem.* **2014**, *16*, 90-95; c) P. Bandyopadhyay, B. Bhattacharya, K. Majhi, P. Majee, U. Sarkar, M. Md. Seikh, *Chem. Phys. Lett.* **2017**, *686*, 88-96.

[15] E. Adler, R. Magnusson, *Acta Chem. Scand.* **1959**, *13*, 505-519.

[16] J. Yang, M. A. Cohen-Stuart, M. Kamperman, *Chem. Soc. Rev.* **2014**, *43*, 8271-8298.

[17] a) F. Nador, F. Novio, D. Ruiz-Molina, *Chem. Commun.* **2014**, *50*, 14570-14572. b) M. A. Moreno-Villaécija, J. Sedó-Vegara, E. Guisasola, A. Baeza, M. Vallet-Regí, F. Nador, D. Ruiz-Molina *ACS Appl. Mater. Interfaces* **2018**, *10*, 7661-7669.

[18] a) F. Meng., X. Li., S. Torker., Y. Shi, X. Shen, A. H. Hoveyda, Nature, **2016**, *537*, 387-393; b) T. A. Mohamed, A. M. Mustafa, W. M. Zoghaib, M. S. Afifi, R. S. Farag, Y. Badr, *J. Mol. Struct. THEOCHEM* **2008**, *868*, 27-36.

[19] a) J. Kumanotani, *Prog. Org. Coat.* **1999**, *26*, 163; b) M. A. ElSohly, P. D. Adawadkar, C. Ma, C. E. Turner, *J. Nat. Prod.* **1982**, *45*, 532-538.

[20] N. N Adarsh, F. Novio, D. Ruiz-Molina, *Dalton Trans.*, **2016**, *45*, 11233-11255.

[21] P. K. Dhal, F. H. Arnold, *Macromolecules* **1992**, *25*, 7051-7059.

[22] J. Park, K. An, Y. Hwang, J.-G. Park, H.-J. Noh, J.-Y. Kim, J.-H. Park, N.-M. Hwang, T. Hyeon, *Nat. Mater.* **2004**, 3, 891-895.

[23] C. Adamo, V. Barone, *J. Chem. Phys.* **1999**, *110*, 6158-6170.

[24] A. Schäfer, C. Huber, R. Ahlrichs, *J. Chem. Phys.* **1994**, *100*, 5829-5835.

[25] a) S. Grimme, J. Antony, S. Ehrlich, H. Krieg, *J. Chem. Phys.* **2010**, *132*, 154104-154119; b) R. Ahlrichs, M. Bär, M. Hacer, H. Horn, C. Kömel, *Chem. Phys. Lett.* **1989**, *162*, 165-169.

[26] J. Tomasi, B. Mennucci, R. Cammi, *Chem. Rev.* **2005**, *105*, 2999-3094.

[27] Gaussian 16, Revision A.03, M. J. Frisch, G. W. Trucks, H. B. Schlegel, G. E. Scuseria, M. A. Robb, J. R. Cheeseman, G. Scalmani, V. Barone, G. A. Petersson, H. Nakatsuji, X. Li, M. Caricato, A. V. Marenich, J. Bloino, B. G. Janesko, R. Gomperts, B. Mennucci, H. P. Hratchian, J. V. Ortiz, A. F. Izmaylov, J. L. Sonnenberg, D. Williams-Young, F. Ding, F. Lipparini, F. Egidi, J. Goings, B. Peng, A. Petrone, T. Henderson, D. Ranasinghe, V. G. Zakrzewski, J. Gao, N. Rega, G. Zheng, W. Liang, M. Hada, M. Ehara, K. Toyota, R. Fukuda, J. Hasegawa, M. Ishida, T. Nakajima, Y. Honda, O. Kitao, H. Nakai, T. Vreven, K. Throssell, J. A. Montgomery, Jr., J. E. Peralta, F. Ogliaro, M. J. Bearpark, J. J. Heyd, E. N. Brothers, K. N. Kudin, V. N. Staroverov, T. A. Keith, R. Kobayashi, J. Normand, K. Raghavachari, A. P. Rendell, J. C. Burant, S. S. Iyengar, J. Tomasi, M. Cossi, J. M. Millam, M. Klene, C. Adamo, R. Cammi, J. W. Ochterski, R. L. Martin, K. Morokuma, O. Farkas, J. B. Foresman, and D. J. Fox, Gaussian, Inc., Wallingford CT, **2016**.

[28] a) J. Contreras-García, E. R. Johnson, S. Keinan, R. Chaudret, J. -P. Piquemal, D. N. Beratan, W. Yang, *J. Chem. Theory Comput.* **2011**, *7*, 625-632; b) R. F. W. Bader, *Chem. Rev.* **1991**, *91*, 893-928; c) AIMAll Version 13.05.06, Todd A. Keith, TK Gristmill Software, Overland Park KS, USA, **2013.**

Entry for the Table of Contents (Please choose one layout)

Layout 1:

FULL PAPER

Text for Table of Contents

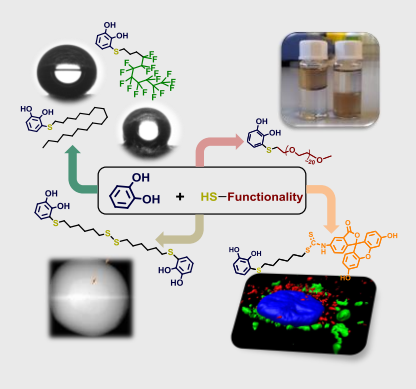

Juan Mancebo-Aracil, Carolina Casagualda, Miguel Ángel Moreno-Villaécija, Fabiana Nador, Javier García-Pardo, Antonio Franconetti-García, Félix Busqué, Ramon Alibés, María José Esplandiu, Daniel Ruiz-Molina, Josep Sedó-Vegara**

Page No. – Page No.

Bioinspired Functional Catechol Derivatives Through Simple Thiol Conjugate Addition